Hydro/engineering shallow geophysical investigation for sustainable development in Ras Muhammed national park, Sinai, Egypt

Mohamed H. Khalil and Sherif M. Hanafy. Geophysics Dept., Faculty of Science, Cairo University.*

Summary

We present the result of a geophysical study at Ras Mohammed national park, south Sinai, Egypt. In this study we recorded eighteen P-wave seismic profiles, and 14 vertical electrical soundings (VESs). Three bore-holes are used as ground truth to constrain the resistivity/seismic inversion. The seismic tomograms and the electric models are used to generate subsurface geological and hydrological models of the area of study. These models are used as a guide to create a better developing plan of the area.

Introduction

In 1980 the Egyptian Environmental Affairs Agency (EEAA) declared Ras Mohammed area as the first reserve area at Egypt for the protection of marine and terrestrial wildlife. It is classified into two parts: marine (parts of Gulf of Suez and Gulf of Aqaba) and terrestrial (Por and Tsurnamal, 1973). The name literally means "Muhammed's Head", where "head" in this instance means "headland". Ras Mohammed national park (RMNP) represents one of the few protected coral reefs and mangrove forest ecosystems in the region. It is an important ecological, economic, social, ecotourism resources and cultural asset for Egypt and beyond. The park contains a variety of stunning geological features, such as uplifted coral reefs, alluvial plains, Wadis, granite, sandstone mountains, and soft dunes (Nir, 1971). Furthermore, it is home to many terrestrial species including foxes, gazelles, reptiles, ibexes and migratory birds such as the white stork. Noteworthy, RMNP has annually hundreds of thousands of visitors (Ibrahim, 2011).

The Egyptian government is preparing a sustainable development master plan for RMNP. Geophysical investigation for the qualitative and quantitative conditions of the freshwater aquifer and shallow soil engineering characteristics constitutes is one of the cornerstones for the planned development. Accordingly, 14 Schlumberger vertical electrical soundings (VESs) (maximum AB/2 = 1000 m), 8 shallow 2D and 10 shallow 2.5D P-wave seismic refraction profiles (355 m each), and borehole data are carried out in the study area to fulfill the targets of the study. The results of the applied geophysical seismic and resistivity techniques were interpreted in an integrated manner.

Geological setting

The area of study (Figures 1) is a part of the Ras Mohammed national park (RMNP) and covers an area of about 311 km^2, lying between longitudes 33.85° and 34.15° E and latitudes 27.80° and 28.05° N. The area is bounded to the east by steep rising mountains and to the west by the Gulf of Suez (average tidal range is 1 m). Climate in the entire area is typical of that arid region. Air temperature varies from 15° C in the short winter to more than 40° C in the summer (Sultan et al., 2009).

RMNP is located in the southern part of El–Qaa plain (Figure 1) which is a secondary rift basin trending NNW-SSE, parallel to the main rift system of the Gulf of Suez (Said, 1990). It is composed of sedimentary rocks (Miocene and post Miocene) and bounded by mountains of igneous and metamorphic Pre-Cambrian rocks which is a part of the Arabian–Nubian shield, and are represented by monzogranites and alkali granites (Shata et al., 1992). RMNP is covered by loose recent deposits of the Quaternary alluvial (El-Refaei, 1984).

The groundwater in the area (south El-Qaa Quaternary alluvial aquifer) is slightly brackish (TDS: 600-900 ppm) (SEAM Programme 1999) and constitutes the main source for the freshwater in the area (Sultan et al., 2009). The salinity of the groundwater is contributed to changes in the groundwater flow system which dissolute salts and leaches stagnant old saline water in the coral reefs body (Khalil, 2012a). Furthermore, intrusion of the Gulf of Suez influences dramatically affect the salinity of the groundwater (Khalil, 2009, 2010, 2012b, 2013).

The predominant flow of the groundwater is from northeast to southwest (Leppard and Gawthorpe, 2006) where the freshwater appears floating over the saltwater (Hammad, 1980; Khalil, 2010, 2012a). Noteworthy, floods occur during the winter when rain water is accumulated in the top of the mountains (Khalil, 2009, 2010). The area is dissected by number of wadis where floods drained and percolated the pronounced alluvial fans fringing the gulf water (Shata et al., 1992). The groundwater potential of this structural basin depends upon the characteristics of the rock units and the recharge conditions (Hammad, 1980). Figure 2 illustrates the subsurface stratigraphic section deduced from the boreholes drilled in the area.

Geoelectric Resistivity Survey

Geoelectrical resistivity is one of the most successful geophysical techniques for investigating groundwater physical properties, especially in a complicated sedimentlogical environment (e. g., Niwas and Singhal, 1981 and Oldenborger et al., 2007). Relationships between

electrical parameters and aquifer characteristics depend on many factors such as lithology, saturation, water content, porosity, and ionic concentration of the pore fluid (e. g., Kelly, 1977 and Asfahani, 2006).

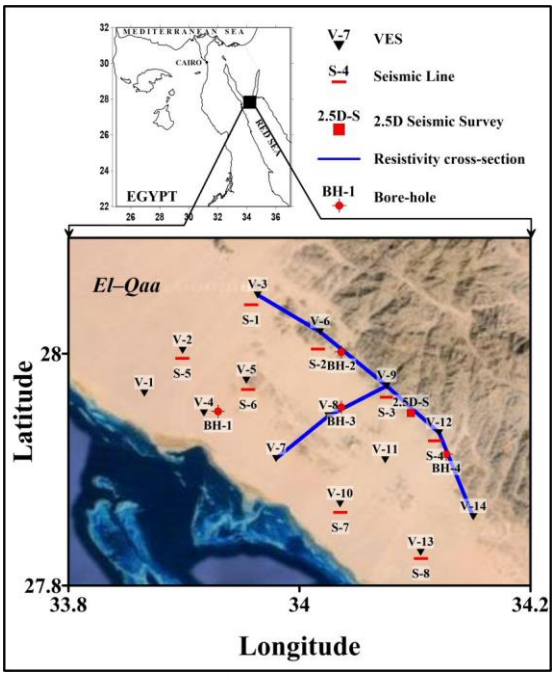

Figure 1: The location of the study area, located at the southern part of Sinai. The location of the electric (VES), 2D seismic, 2.5D seismic, and bore-holes are shown on the map. The blue lines are the electric cross sections constructed from the VESs.

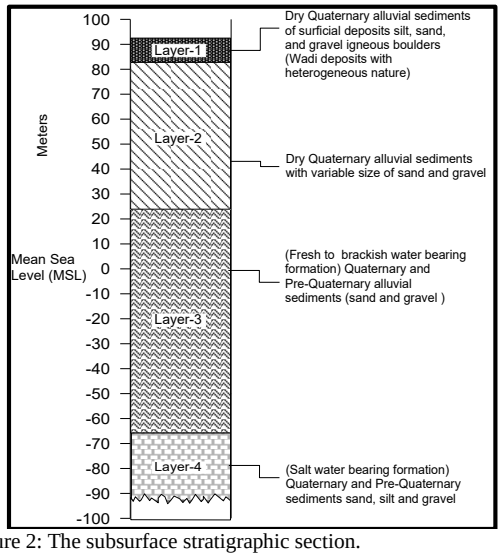

Figure 2: The subsurface stratigraphic section.

Direct current (DC) vertical electrical soundings (VES) method measures the apparent resistivity (ρ_a) of the subsurface (Oldenborger et al., 2007; Khalil, 2013) using Schlumberger configuration. The recorded data is then inverted to develop a 1D model of the subsurface structure and stratigraphy in terms of its electrical properties at each VES (e. g., Halihan et al., 2005; Descloitres et al., 2008). Noteworthy, it is very necessary to calibrate the observed VES data with the available borehole data to assign proper resistivity ranges for the various lithologic units and resolve possible ambiguities in interpretation (Khalil, 2012a,b).

Fourteen Schlumberger VESs with maximum current electrode half-spacing (AB/2) of 1,000 meters were carried out in the study area (Figure 1). This spacing was adequate to investigate the target layer of the freshwater (Quaternary and Pre-Quaternary alluvial) (Figure 2). Resistivity measurements were carried out using a digital signal-enhancement resistivity-meter (ABEM-TERRAMETER, SAS 4000). VES-4, 6, 8 and 12 were conducted close to available water boreholes in order to calibrate the acquired measurements.

Field data were processed and inverted by the methodology discussed by Khalil, 2012a and geoelectric modeling was carried out by IPI2Win (Bobachev, 2002). The maximum root mean square (RMS) error of the resulting models was 5% (Figure 3). Furthermore, the interpreted VES stations, geological subsurface studies, and borehole data in the study area were integrated to produce two geoelectric cross-sections profile-1 and 2 (Figures 4a and 4b).

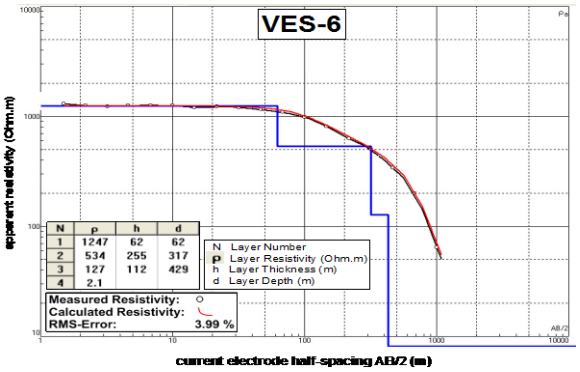

Figure 3: One example, VES 6, of the processed and inverted electric measurements (red line). In this example, 4 subsurface layers are shown (blue line) with resistivity values 1247, 534, 127, and 2.1 Ohm.m and thickness of 62, 255, and 112 m.

Seismic Survey

The recorded seismic data consist of eight profiles (S-1 to S-8 shown in Figure 1) each profile has 72 common shot gathers with 72 receivers per shot gather. The shot/receiver intervals are 5 meters, profile length is 355 m, and to enhance the signal to noise ratio of the recorded data, we

used 15 to 20 stacks at each shot location. An accelerated weight-drop, 40 kg, is used as the seismic source.

The first arrival traveltimes of all recorded traces are picked, and then the picked traveltimes are inverted using traveltime tomography to generate the velocity tomogram (Nemeth et al., 1997). The final tomograms after 40 iterations are shown in Figure 5 for profiles S-1 and S-3.

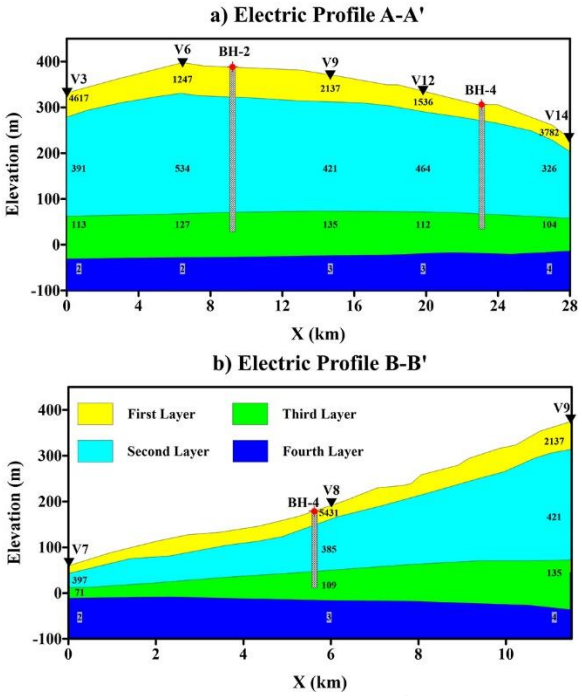

Figure 4: Two cross sections constructed from the resistivity measurements, their locations are shown on Figure 1 as blue lines. Four different layers are shown on the cross sections, they are: (1) Dry Quaternary alluvium sediments of silt, sand, and gravel boulders with resistivity range 1247 - 5437 Ohm.m. (2) Dry Quaternary alluvium sediments with variable size of sand and gravel with resistivity range 326 - 534 Ohm.m. (3) Quaternary and pre-Quaternary alluvium sediments, the fresh to brackish water bearing formation, with resistivity range 56 - 135 Ohm.m. (4) Quaternary and pre-Quaternary sand- and silt-stone, salt water bearing formation. With resistivity range 1 - 5 Ohm.m.

Figure 5 shows two tomogram examples, the first is away from the faulted zone, while the second is at the faulted zone.

A local low velocity anomaly, called colluvial wedge, is shown in Figure 5b, a similar one is also shown on the tomogram of profile S-4 (not shown in this abstract), while the other tomograms S1, S2, and S5 to S-8 don't show a similar anomaly. Such colluvial wedges are usually associated with normal faults (Hanafy et al., 2015; Hanafy, 2012; McCalpin, 1996), to get a better understanding of this anomaly, we recorded another ten parallel 2D seismic profiles between the location of profile S-3 and S-4. We also used 72 shot gather, with 72 receiver per shot gather and 5 meters shot/receiver intervals. The distance between each two lines is 10 m. The first arrivals traveltimes of the new 10-profiles are picked and inverted to create 10 tomograms, which then used to obtain a pseudo 3D image shown in Figure 6. We called the image in Figure 6 pseudo 3D or 2.5D since it is not a true 3D image, in a true 3D image we should shot in the cross-line direction, however in our experiment we shot only in the in-line direction. The 2.5D image (Figure 6) shows the extension of the faults in the third dimension (Y-dimension).

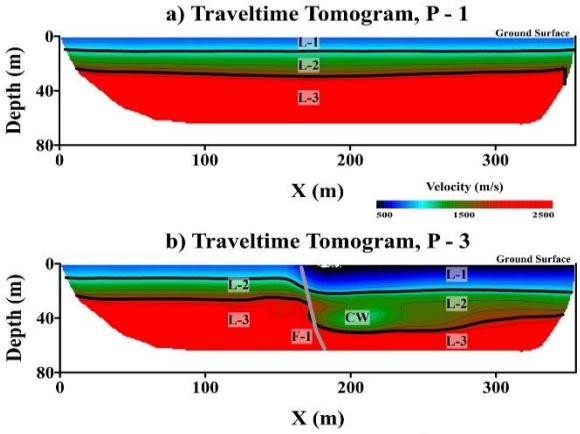

Figure 5: Two traveltime tomograms obtained from the recorded seismic data at locations 1 and 3, respectively.

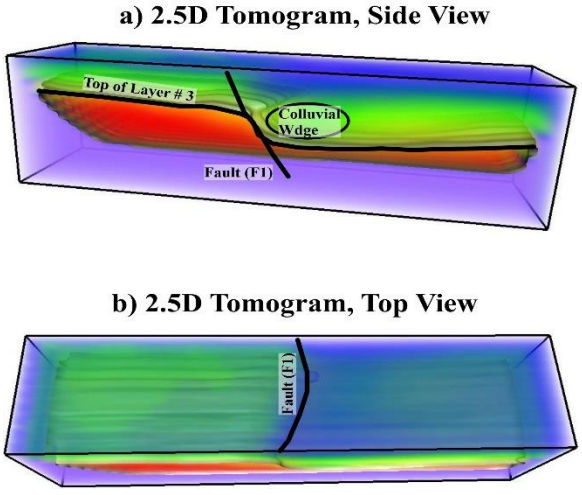

Figure 6: The 2.5D image of the recorded seismic data, where a) is a side view, and b) is a top view. The colluvial wedge in this image refers to the location of the subsurface fault.

Results and Discussion

Resistivity: Figure 3 illustrates one sample (VES-6) of the inverted resistivity data which correlated with the adjacent borehole (BH-2) (Figure 2). Figures 4a and 4b exhibit geoelectric cross-sections; profile-1 and 2, respectively. A general four electric-subsurface layers were recognized in the area, from top to bottom as follows:

1. A surface layer characterized by mixture of dry Quaternary alluvium sediments silt, sand, and gravel igneous boulders (Wadi deposits with heterogeneous nature). This layer characterized by resistivities ranged from 1247 to 5437 Ω.m and thickness ranged from 3 to 64 m.
2. A second layer characterized by dry Quaternary alluvium sediments of sand and gravel with variable size. This layer characterized by resistivities ranged from 326 to 534 Ω.m and thickness ranged between 13 and 255 m.
3. A third layer of Quaternary and Pre-Quaternary alluvium sediments (sand and gravel). This layer represents the fresh aquifer and characterized by resistivities ranged from 56 to 135 Ω.m and thickness ranged between 11 and 112 m.
4. A fourth bottom layer represents the salt water bearing formation of Quaternary and Pre-Quaternary sediments of silt, sand, and gravel. The resistivities of this layer were very low and ranged between 1.7 and 4.3 Ω.m.

The fresh/saline water interface was successfully depicted from the resistivity measurements. The relatively freshwater aquifer (slightly brackish) floats over the deeper saline groundwater. The depth to the top of the fresh aquifer ranged between 15 and 319 m. Depth increased gradually toward the northeast direction and reached maximum at VES-6. The highest thickness of the fresh aquifer was attained toward the northeast direction at VES-6 (112 m) and gradual decrease toward the western part could be observed. The lowest thickness of the aquifer was attained at VES-4 (23 m). The aquifer true resistivity increased gradually toward the northeast direction and reached maximum 135 Ohm.m at VES-9.

Seismic: In the seismic survey 4 units are shown. They can be described from top to bottom as follow:

1. The surface layer has a P-wave velocity values of 650 – 850 m/s with thickness of 11 m (Figure 5a), while the P-wave velocity at the faulted zone ranges between 400 and 850 m/s and the thickness increased to 20 m (Figure 5b). This layer is corresponding to the Quaternary alluvium sediments (layer 1 in the resistivity sections).
2. The second layer has a P-wave velocity range of 1050 – 1600 m/s with an average thickness of 19 m. This layer is corresponding to a dry Quaternary alluvium sediments of sand and gravel.
3. The third layer has a P-wave velocity larger than 2200 m/s and corresponding to dry Quaternary sediments (the second layer in the resistivity section).
4. A local low-velocity anomaly corresponding to a colluvial wedge associated with the normal fault. This unit is only shown at seismic sections recorded at the faulted zones (profiles 3 and 4, and the 2.5D survey).

The aquifer is not shown in the seismic sections since it is deeper than the maximum depth of investigation reached by the seismic profiles.

Conclusions

In this study both resistivity and seismic methods are used to explore the subsurface geology and hydrology at the area of study. The resistivity method is mainly used to find the depth to and the thickness of the water aquifer. Resistivity result show that the water aquifer is split into two parts, the upper is a fresh-brackish and the lower is a saline water bearing formation.

The seismic method is used to explore the geological and structural subsurface condition. Three different subsurface layer and one normal fault is found at the area of study. The groundwater is not shown on the seismic tomograms since the depth of penetration of the seismic data is shallower than the aquifer.

EDITED REFERENCES

Note: This reference list is a copyedited version of the reference list submitted by the author. Reference lists for the 2016 SEG Technical Program Expanded Abstracts have been copyedited so that references provided with the online metadata for each paper will achieve a high degree of linking to cited sources that appear on the Web.

REFERENCES

Asfahani, J., 2006, Neogene aquifer properties specified through the interpretation of electrical sounding data, Salamiyeh Region, Central Syria. Hydrological Processes, **21**, 2934–2943.

Bobachev, C., 2002, IPI2Win: A windows software for an automatic interpretation of resistivity sounding data, Ph.D.: Moscow State University.

Descloitres, M., O. Ribolzi, Y. Le Troquer, and J. P. Thiébaux, 2008, Study of water tension differences in heterogeneous sandy soils using surface ERT: Journal of Applied Geophysics, **64**, 83–98, http://dx.doi.org/10.1016/j.jappgeo.2007.12.007.

El-Refaei, A. A., 1984, Geomorphological and hydrogelogical studies on El-Qaa plain, Gulf of Suez, Sinai, Egypt. M. Sc. Thesis, Faculty of Science Cairo University, 298.

Halihan, T., S. Paxton, I. Graham, T. Fenstemakerb, and M. Rileya, 2005, Post-remediation evaluation of a LNAPL site using electrical resistivity imaging: Journal of Environmental Monitoring, **7**, 283–287, http://dx.doi.org/10.1039/b416484a.

Hammad, F. A., 1980, Geomorphological and hydrogeological aspects of Sinai Peninsula, A.R.E. Annals of the geological Survey of Egypt Volume X, 807–817.

Hanafy, Sh., 2012, Subsurface fault and colluvial wedge detection using resistivity, refraction tomography and seismic reflection. EAGE meeting: Copnhagen, Denemark.

Hanafy, Sh. M., A. Mattson, R. L. Bruhn, S. Liu, and G. T. Schuster, 2015, Outcrops and well logs as a practicum for calibrating the accuracy of traveltime tomograms: Interpretation (Tulsa), **3**, SY27–SY40, http://dx.doi.org/10.1190/INT-2014-0217.1.

Ibrahim, F. N., 2011, An Economic Geography: I. B. Tauris & Company, 194.

Kellys, W. E., 1977, Geoelectrical sounding for estimating aquifer hydraulic conductivity: Ground Water, **15**, 420–425, http://dx.doi.org/10.1111/j.1745-6584.1977.tb03189.x.

Khalil, M. H., 2009, Hydrogeophysical assessment of Wadi El-Sheikh aquifer, Saint Katherine, South Sinai, Egypt: Journal of Environmental & Engineering Geophysics, **14**, 77–86, http://dx.doi.org/10.2113/JEEG14.2.77.

Khalil, M. H., 2010, Hydro-geophysical configuration for the quaternary aquifer of Nuweiba alluvial fan: Journal of Environmental and Engineering Geophysics, **15**, 77–90, http://dx.doi.org/10.2113/JEEG15.2.77.

Khalil, M. H., 2012a, Reconnaissance of freshwater conditions in a coastal aquifer: synthesis of 1D geoelectric resistivity inversion and geohydrological analysis: Near Surface Geophysics, **10**, 427–441.

Khalil, M. H., 2012b, Magnetic, geo-electric, and groundwater and soil quality analysis over a landfill from a lead smelter, Cairo, Egypt: Journal of Applied Geophysics, **86**, 146–159, http://dx.doi.org/10.1016/j.jappgeo.2012.08.004.

Khalil, M. H., 2013, Detection of magnetically susceptible Dyke Swarms in a fresh coastal aquifer: Pure and Applied Geophysics, **170**, 1–17.

Leppard, C. W., and R. L. Gawthorpe, 2006, Sedimentology of rift climax deep water systems; Lower Rudeis Formation, Hammam Faraun Fault Block, Suez Rift, Egypt: Sedimentary Geology, **191**, 67–87, http://dx.doi.org/10.1016/j.sedgeo.2006.01.006.

Lois, I. F., G. A. Karantonis, N. S. Voulgaris, and F. I. Louis, 2004, The contribution of geophysical methods in the determination of aquifer parameters: The case of Mornos River delta, Greece: Research Journal of Chemistry and Environment, **8**, 41–49.

McCalpin, J. P., 1996, Paleoseismology: Academic Press.
Nemeth, T., E. Normark, and F. Qin, 1997, Dynamic smoothing in crosswell traveltime tomography: Geophysics, **62**, 168–176, http://dx.doi.org/10.1190/1.1444115.
Nir, D., 1971, Marine terraces of southern sinai: Geographical Review, **61**, 32–50 (American Geographical Society), http://dx.doi.org/10.2307/213366.
Niwas, S., and D. C. Singhal, 1981, Estimation of aquifer tranmissivity from Dar Zarrouk parameters in porous media: Hydrology, **50**, 393–399, http://dx.doi.org/10.1016/0022-1694(81)90082-2.
Oldenborger, G. A., M. D. Knoll, P. S. Routh, and D. J. Labrecque, 2007, Time-lapse ERT monitoring of an injection/withdrawal experiment in a shallow unconfined aquifer: Geophysics, **72**, no. 4, F177–F187, http://dx.doi.org/10.1190/1.2734365.
Por, F. D., and M. Tsurnamal, 1973, Ecology of the Ras Muhammad Crack in Sinai: Nature, **241**, 43–44, http://dx.doi.org/10.1038/241043b0.
Said, R., 1990, Geology of Egypt: Balkema, p. 722.
Programme, S. E. A. M., 1999, South Sinai environmental and development profile: Egyptian Environmental Affairs Agency, P. 28.
Shata, A. M. M., M. S. El Shazli, T. A. Diab, L. Abdel, and M. A. Tamer, 1992, Preliminary report on the groundwater resources in the Sinai Peninsula, Egypt, Parts I and II: The Desert Institute, Water Resources Department, 92–105.
Sultan, A. S., I. M. Mahmoud, and M. S. Fernando, 2009, Hydrogeophysical study of the El Qaa Plain, Sinai, Egypt: Bulletin of Engineering Geology and the Environment, **68**, 525–537, http://dx.doi.org/10.1007/s10064-009-0216-z.